Title	Numerical solution of cracked thin plates subjected to bending, twisting and shear loads
Author(s)	Su, RKL; Sun, HY
Citation	International Journal Of Fracture, 2002, v. 117 n. 4, p. 323-335
Issued Date	2002
URL	http://hdl.handle.net/10722/48535
Rights	The original publication is available at www.springerlink.com

Paper submitted to the International Journal of Fracture, Dec 2001, revised in July 2002.

NUMERICAL SOLUTION OF CRACKED THIN PLATES SUBJECTED TO BENDING, TWISTING AND SHEAR LOADS

R.K.L. Su[a,1], and H.Y. Sun[b]

[a] Assistant Professor, Department of Civil Engineering, The University of Hong Kong, Pokfulam Road, Hong Kong, PRC

[b] Research Student, Department of Civil Engineering, The University of Hong Kong, Pokfulam Road, Hong Kong, PRC

[1] Corresponding Author : Fax (852) 2559 5337
: e-mail address klsu@hkucc.hku.hk

Total Number of Pages: 23

Number of Figures: 9

Abstract

A semi-analytical method namely fractal finite element method is presented for the determination of mode I and mode II moment intensity factors for thin plate with crack using Kirchhoff's theory. Using the concept of fractal geometry, infinite many of finite elements is generated virtually around the crack border. Based on the analytical global displacement function, numerous degrees of freedom (DOF) are transformed to a small set of generalised coordinates in an expeditious way. The stress intensity factors can be obtained directly from the generalized coordinates. No post-processing and special finite elements are required to develop for extracting the stress intensity factors. Examples of cracked plate subjected to bending, twisting and shear loads are given to illustrate the accuracy and efficiency of the present method. The influence of finite boundaries on the calculation of the moment intensity factors is studied in details. Very accuracy results when compare with the theoretical and numerical counterparts are found.

Key words

Thin plate, crack, stress intensity factors, eigenfunction expansion, fractal, finite element, Kirchhoff's theory.

1. Introduction

Theoretical analysis of bending problems of cracked plates under the framework of classical plate theory has been examined in the past, although less extensively than the case of stretching. Such analysis was first carried out using the complex variable technique by Williams (1961). He obtained the general stress distribution in the vicinity of the crack tip for plates loaded in bending, and found that the stress was proportional to the inverse of the square root of the radial distance from the crack tip. Sih *et al*. (1962) used Williams' results to define symmetric and anti-symmetric stress intensity factors for cracked infinite plate problems involving bending loads. Furthermore, they analytically solved an infinite plate with crack subjected to bending, twisting and shear loads. Those solutions were incorporated in the stress intensity factor handbook by Murakami (1987). However, Zehnder and Hui (1994) reconsidered those problems and found some errors in the solutions of cracks subjected to shearing and twisting loads. By using the conformal mapping method, the stress intensity factors for the uniform far-field shearing problem were found to be $k_1 = \dfrac{3Q_0 a^{3/2} \nu \cos\beta}{h^2}$ and $k_2 = \dfrac{3Q_0 a^{3/2} \sin\beta}{h^2}$. In the case of pure twisting, none of the stresses closed to crack tip were found to be singular, thus k_1 and k_2 are both equal to zero. The numerical solutions by Hui and Zehnder (1993) and Zucchini *et al*.(2000) also concurred with Zehnder's solutions.

To deal with more realistic problems with complicated boundary conditions for plates with cracks, numerical approaches appear to be imperative. Wilson and Thompson (1971) first calculated the symmetric bending stress intensity factor by means of crack tip deflections for a finite rectangular plate containing a centre crack, subjected to pure cylindrical bending by conventional finite element method. Ahmad and Loo (1979) developed a singular crack tip plate element and solved the problem of plate containing inclined central crack subjected to bending load. It is noted that the calculated stress intensity factors for both k_1 and k_2 were closely agreed with Sih's solution despite that errors in the k_2 solutions were found later by Zehnder and Hui (1994). Chen and Chen (1984) employed the hybrid-displacement finite element procedure using the singular elements embedded with crack-tip singularity to solve various boundary configurations of thin cracked plates under bending. However, anti-symmetric bending stress intensity factor k_2 was found not to be zero regardless the pure symmetrical problem of square center-cracked plate subjected to edge bending moment. Park

and Atluri (1999), Chen and Shen (1993) and Chen *et al*. (1992) used the finite element alternating approach to solve the problems of plates with single and multiple cracks. Only Chen and Shen actually considered the mixed mode plate bending problem by using the anti-symmetric bending stress intensity factor derived from Sih *et al*. (1962). However, their results were found to be concurred with these of Sih but inconsistent with Zehnder's solutions.

According to these surveys, most of the researcher can accurately predict the symmetric moment intensity factor but not the anti-symmetric moment intensity factor. The investigation of a reliable and accurate numerical method to solve thin plate with mixed mode crack by numerical method is imperative. It is our attention to extend the fractal finite element method (FFEM) [Leung and Su, 1996] to solve thin cracked plate subjected to bending, twisting and shear loads. The FFEM combines the advantages of the finite element method and the efficiency of the fractal transformation technique to model the regular and singular behavior of cracked plates. To demonstrate the accuracy and reliability of this technique for both mode I and mode II problems, numerical examples concerning thin plates, with single crack, subjected to bending, shear and twisting are analyzed. The influence of finite boundaries on the computation of moment intensity factors is studied in detail.

2. Global interpolation function

In the absence of the transverse loading, Timoshenko and Woinowsky-Krieger (1959) derived the appropriate differential equation controlling the deflection $w = w(r, \theta)$ of thin plate as

$$\nabla^2 \nabla^2 w = 0 . \tag{1}$$

where $\nabla^2 = \frac{\partial^2}{\partial r^2} + \frac{1}{r}\frac{\partial}{\partial r} + \frac{1}{r^2}\frac{\partial^2}{\partial \theta^2}$ is the Laplacian. The moments M_r, M_θ and $M_{r\theta}$ and shears Q_r and Q_θ can be related with the deflection w as follows

$$M_r(r,\theta) = -D\left[\frac{\partial^2 w}{\partial r^2} + \nu\left(\frac{1}{r}\frac{\partial w}{\partial r} + \frac{1}{r^2}\frac{\partial^2 w}{\partial \theta^2}\right)\right] \tag{2}$$

$$M_\theta(r,\theta) = -D\left[\frac{1}{r}\frac{\partial w}{\partial r} + \frac{1}{r^2}\frac{\partial^2 w}{\partial \theta^2} + \nu\frac{\partial^2 w}{\partial r^2}\right] \tag{3}$$

$$M_{r\theta}(r,\theta) = (1-\nu)D\left[\frac{1}{r}\frac{\partial}{\partial\theta}\left(\frac{\partial w}{\partial r} - \frac{w}{r}\right)\right] \tag{4}$$

$$Q_r(r,\theta) = -D\frac{\partial}{\partial r}(\nabla^2 w) + \frac{1}{r}\frac{\partial}{\partial\theta}(M_{r\theta}) \tag{5}$$

$$Q_\theta(r,\theta) = -D\frac{1}{r}\frac{\partial}{\partial\theta}(\nabla^2 w) + \frac{\partial}{\partial r}(M_{r\theta}) \tag{6}$$

in which $D = \dfrac{Eh^3}{12(1-\nu^2)}$ is the flexural rigidity, E is the Young's modulus and ν is the Poisson's ratio. Assuming the traction-free boundary conditions at the crack faces, one has the boundary conditions,

$$M_\theta = Q_\theta = 0 \quad \text{for} \quad \theta = \pm\pi\,. \tag{7}$$

It has been shown by Williams (1961) that the desired characteristic solutions are of the form

$$\begin{aligned}(1-\nu)Dw_n(r,\theta) = a_0^{(3)} + r^{(n+2)/2}\Big[&a_n^{(1)}\cos(n/2-1)\theta + a_n^{(2)}\sin(n/2-1)\theta \\ &+ b_n^{(1)}\cos(n/2+1)\theta + b_n^{(2)}\sin(n/2+1)\theta\Big] \quad (\text{For} \quad n = 0,1,2,...)\end{aligned} \tag{8}$$

where $a_0^{(3)}$, $a_n^{(i)}$ and $b_n^{(i)}$ ($i = 1$ and 2) are the arbitrary constants. The relations between the constants are found by substituting equation (8) into (7) to yield

$$b_n^{(1)} = a_n^{(1)}\frac{(n+2)(1-\nu)}{(-n+(-1)^n 6)+(n+(-1)^n 2)\nu} \tag{9}$$

and

$$b_n^{(2)} = a_n^{(2)}\frac{(n+2)(1-\nu)}{(-n-(-1)^n 6)+(n-(-1)^n 2)\nu}\,. \tag{10}$$

By neglecting the shear deformation, one has the rotational displacements

$$\psi_r = \frac{\partial w}{\partial r} \quad \text{and} \quad \psi_\theta = \frac{1}{r}\frac{\partial w}{\partial\theta}. \tag{11}$$

Substituting equations (9) and (10) into (8) and then into (11), one has the displacement distribution in the vicinity of the end of crack

$$\psi_{rn} = \frac{r^{n/2}}{2(1-\nu)D} \times$$
$$\left\{ a_n^{(1)} \left[(n+2)\cos(n/2+1)\theta + \frac{(n+2)^2(1-\nu)}{(-n+(-1)^n 6)+(n+(-1)^n 2)\nu} \cos(n/2-1)\theta \right] \right. \tag{12}$$
$$\left. + a_n^{(2)} \left[(n+2)\sin(n/2+1)\theta + \frac{(n+2)^2(1-\nu)}{(-n-(-1)^n 6)+(n-(-1)^n 2)\nu} \sin(n/2-1)\theta \right] \right\}$$

$$\psi_{\theta n} = -\frac{r^{n/2}}{2(1-\nu)D} \times$$
$$\left\{ a_n^{(1)} \left[(n+2)\sin(n/2+1)\theta + \frac{(n^2-4)(1-\nu)}{(-n+(-1)^n 6)+(n+(-1)^n 2)\nu} \sin(n/2-1)\theta \right] \right. \tag{13}$$
$$\left. - a_n^{(2)} \left[(n+2)\cos(n/2+1)\theta + \frac{(n^2-4)(1-\nu)}{(-n-(-1)^n 6)+(n-(-1)^n 2)\nu} \cos(n/2-1)\theta \right] \right\}$$

$$w_n = \frac{r^{(n+2)/2}}{(1-\nu)D} \times$$
$$\left\{ a_n^{(1)} \left[\cos(n/2+1)\theta + \frac{(n+2)(1-\nu)}{(-n+(-1)^n 6)+(n+(-1)^n 2)\nu} \cos(n/2-1)\theta \right] \right. \tag{14}$$
$$\left. + a_n^{(2)} \left[\sin(n/2+1)\theta + \frac{(n+2)(1-\nu)}{(-n-(-1)^n 6)+(n-(-1)^n 2)\nu} \sin(n/2-1)\theta \right] \right\}$$

Furthermore, the displacement distribution (ψ_1, ψ_2, w) in the rectangular coordinate system as shown in Figure 1 is given by the transformation,

$$\begin{Bmatrix} \psi_1 \\ \psi_2 \\ w \end{Bmatrix} = \begin{bmatrix} \cos\theta & -\sin\theta & 0 \\ \sin\theta & \cos\theta & 0 \\ 0 & 0 & 1 \end{bmatrix} \begin{Bmatrix} \psi_r \\ \psi_\theta \\ w \end{Bmatrix}. \tag{15}$$

Equation (15) represents a generalized displacement distribution in the vicinity of a crack tip. It will be used as the global interpolating function for the displacement field near the crack tip.

Using the definitions of bending stress intensity factors for cracked plate by Sih *et al*. (1962), the moment intensity factors K_1 and K_2 are defined as follows,

$$K_1 = \lim_{r \to 0} \sqrt{2r}\, M_{22}(r,0)$$

$$K_2 = \lim_{r\to 0}\left(\frac{3+\nu}{1+\nu}\right)\sqrt{2r}M_{12}(r,0)\,. \tag{16}$$

Those factors can be obtained by substituting equation (14) into equations (3) and (6) and putting $\theta = 0$ and $r \to 0$, i.e.,

$$K_1 = \frac{3\sqrt{2}(3+\nu)}{(7+\nu)}a_1^{(1)} \quad \text{and} \qquad K_2 = \frac{3\sqrt{2}(3+\nu)}{(5+3\nu)}a_1^{(2)}. \tag{17}$$

Therefore, the evaluation of moment intensity factors is directly reduced to the determination of the two coefficients $a_1^{(1)}$ and $a_1^{(2)}$. No post-analysis and extrapolation are needed.

3. DKT plate elements with similar shape

The properties of plate bending elements with similar shapes as shown in Figure 2 will be explored here. A triangular 9 DOF element, namely a discrete Kirchhoff theory (DKT) element by Stricklin *et al*. (1969) is chosen for the subsequent fractal transformation. Considering two elements, denoted by *1* and *k*, having similar shapes of length ratio $L_k / L_1 = \bar{\xi}^{(k-1)}$ where $0 < \bar{\xi} < 1$, the stiffness matrices for the element k can be expressed as,

$$\mathbf{K}^k = \begin{bmatrix} \mathbf{K}_{11}^k & \mathbf{K}_{12}^k & \mathbf{K}_{13}^k \\ & \mathbf{K}_{22}^k & \mathbf{K}_{23}^k \\ sym & & \mathbf{K}_{33}^k \end{bmatrix}. \tag{18}$$

Any sub-matrix in $\mathbf{K}^k$ may be related to that of $\mathbf{K}^1$ [Leung and Su, 1996] as follows:

$$\mathbf{K}_{ij}^k = \begin{bmatrix} k_{\psi_1\psi_1}^1 & k_{\psi_1\psi_2}^1 & \frac{1}{\bar{\xi}^{(k-1)}}k_{\psi_1 w}^1 \\ k_{\psi_2\psi_1}^1 & k_{\psi_2\psi_2}^1 & \frac{1}{\bar{\xi}^{(k-1)}}k_{\psi_2 w}^1 \\ \frac{1}{\bar{\xi}^{(k-1)}}k_{w\psi_1}^1 & \frac{1}{\bar{\xi}^{(k-1)}}k_{w\psi_2}^1 & \frac{1}{\bar{\xi}^{2(k-1)}}k_{ww}^1 \end{bmatrix}_{ij} ;(i=j=1,2,3) \tag{19}$$

Equation (19) can be used to calculate stiffness coefficients of any DKT element with geometric similarity.

4. Fractal transformation method

The FFEM is based on the separation of the singular domain and the regular domain from a cracked plate alone an artificial surface boundary Γ_0 as displayed in Figure 3. Within the singular region, solution is obtained by the FFEM, and inside the regular domain, it is obtained by conventional FEM technique. The generalized stiffness matrix in the singular domain is evaluated by transforming the stiffness matrix of the first layer of mesh (in Figure 4) and modifying each element in this matrix accordingly.

For the first layer of fractal mesh, as only $\mathbf{d}_s$ (the DOF of the slave nodes which are nodes other than master nodes as shown in Figure 4) will be transformed, the global interpolation of displacements can be written as follows:

$$\begin{Bmatrix} \mathbf{d}_s \\ \mathbf{d}_m \end{Bmatrix} = \begin{bmatrix} \mathbf{T}_s^f & \mathbf{0} \\ \mathbf{0} & \mathbf{I} \end{bmatrix} \begin{Bmatrix} \mathbf{a} \\ \mathbf{d}_m \end{Bmatrix} \tag{20}$$

where $\mathbf{I}$ is the identity matrix, $\mathbf{T}_s^f = \mathbf{T}_s^f(r,\theta)$ is the transformation matrix that can be evaluated from the displacement eigenfunctions using equations (12-15), $\mathbf{a}$ is the corresponding generalized coordinates vector of $\mathbf{T}_s^f$ and $\mathbf{d}_m$ denotes the DOF of master nodes of the first layer of fractal mesh. The generalized stiffness matrix for the first layer may be expressed as,

$$\begin{bmatrix} \overline{\mathbf{K}}_{aa} & \overline{\mathbf{K}}_{am} \\ \overline{\mathbf{K}}_{ma} & \mathbf{K}_{mm} \end{bmatrix} = \begin{bmatrix} \mathbf{T}_s^{fT} \mathbf{K}_{ss} \mathbf{T}_s^f & \mathbf{T}_s^{fT} \mathbf{K}_{sm} \\ \mathbf{K}_{ms} \mathbf{T}_s^f & \mathbf{K}_{mm} \end{bmatrix} \tag{21}$$

For inner layers of fractal mesh, each element stiffness matrix within the first layer is transformed and assembled. Based on self-similarity (fractal) concept, infinite number of elements with similar shapes and numerous DOF will be generated near the crack tip with proportional factor of $\bar{\xi}$ as illustrated in Figure 4. The fractal transformation method as described in details by Su *et al*. (2001) will be used to transform and assemble infinitely many layers of mesh. The principle of this method will be explained herein.

For inner layers, all the rotational and translational DOF will be transformed to the corresponding generalized coordinates $\mathbf{a}$. Following equations (12-15), the transformation functions may be written in matrix form $\mathbf{T}^k$ for a triangular element at the kth inner layer, such

that $\mathbf{T}^k = \begin{bmatrix} \mathbf{T}_1^k & \mathbf{T}_2^k & \mathbf{T}_3^k \end{bmatrix}^T$ where the subscripts (1,2 and 3) stand for the 3 nodes of the triangular element. By comparing the transformation matrices of the 1st and k*th* layers of the mesh, the sub-matrix $\mathbf{T}_l^k$ (l=1,2 and 3) can further be related to the corresponding counterparts of the first layer by using the variable $\bar{\xi}$. Hence, the sub-matrix $\mathbf{T}_l^k$ becomes,

$$\mathbf{T}_l^k = \begin{bmatrix} \mathbf{T}_{\psi_1}^f \\ \mathbf{T}_{\psi_2}^f \\ \bar{\xi}^{(k-1)}\mathbf{T}_w^f \end{bmatrix}_l \mathbf{Diag}\left[\alpha_j\left(\bar{\xi}\right)\right] \tag{22}$$

and $\alpha_j(\bar{\xi}) = \bar{\xi}^{n_j(k-1)/2}$ and $n_j = \begin{cases} j/2 & \text{for} \quad j = 1,3,5,\cdots \\ (j-1)/2 & \text{for} \quad j = 2,4,6,\cdots \end{cases}$ (23)

in which $\mathbf{T}_{\psi_1}^f, \mathbf{T}_{\psi_2}^f$ and $\mathbf{T}_w^f$ represent the transformation functions of the rotational (ψ_1 and ψ_2) and vertical (w) displacements, respectively, of the 1st layer.

The generalized stiffness matrix of k*th* layer is given as

$$\begin{aligned} \overline{\mathbf{K}}^k &= \mathbf{T}^{k\,T}\mathbf{K}^k\mathbf{T}^k \\ &= \begin{bmatrix} \mathbf{T}_1^k \\ \mathbf{T}_2^k \\ \mathbf{T}_3^k \end{bmatrix}^T \begin{bmatrix} \mathbf{K}_{11}^k & \mathbf{K}_{12}^k & \mathbf{K}_{13}^k \\ & \mathbf{K}_{22}^k & \mathbf{K}_{23}^k \\ sym & & \mathbf{K}_{33}^k \end{bmatrix} \begin{bmatrix} \mathbf{T}_1^k \\ \mathbf{T}_2^k \\ \mathbf{T}_3^k \end{bmatrix} \end{aligned} \tag{24}$$

By substituting equations (19) and (22) into equation (24), one can express the k^{th} layer of matrix in terms of the 1st layer matrix,

$$\overline{\mathbf{K}}^k = \mathbf{Diag}\left[\alpha_i\right]\mathbf{T}^{f\,T}\mathbf{K}^f\mathbf{T}^f\mathbf{Diag}\left[\alpha_j\right]. \tag{25}$$

Superimposing the stiffness matrices from the 2nd layer to infinite layer, one has the generalized stiffness matrix $\overline{\mathbf{K}}^i$

$$\overline{\mathbf{K}}^i = \sum_{k=2}^{\infty}\overline{\mathbf{K}}^k = \sum_{k=2}^{\infty}\mathbf{Diag}[\alpha_i]^T\,\mathbf{T}^{f\,T}\mathbf{K}^f\mathbf{T}^f\mathbf{Diag}[\alpha_j]. \tag{26}$$

All the entries in the generalized stiffness matrix $\overline{\mathbf{K}}^i$ of equation (26) are geometric series, therefore, it can be further simplified as

$$\overline{\mathbf{K}}^i = \begin{bmatrix} & \vdots & \\ \cdots & \overline{\alpha}_{ij}\overline{k}_{ij}^f & \cdots \\ & \vdots & \end{bmatrix} \tag{27}$$

where $\overline{\alpha}_{ij}(\overline{\xi}) = \dfrac{1}{\overline{\xi}^{-(m_i+n_j)/2} - 1}$ and $m_i = \begin{cases} i/2 & \text{for} \quad i = 1,3,5,\cdots \\ (i-1)/2 & \text{for} \quad i = 2,4,5,\cdots \end{cases}$ (28)

In short, equation (27) indicates that the generalized inner layer stiffness matrices can be evaluated by simply evaluation of the generalized stiffness matrix of 1st layer (by standard matrix transformation method) and modifying each entry $\overline{k}_{ij}^f$ of the matrix in turn by a scale factor $\overline{\alpha}_{ij}$ shown in equation(28). The proportional factor $\overline{\xi}$ of $1/2$ will be used in the subsequent numerical studies. The generalized stiffness matrix of the singular region can be obtained by adding up equations (21) and (27), therefore

$$\begin{bmatrix} \overline{\mathbf{K}}_{aa} + \overline{\mathbf{K}}_i & \overline{\mathbf{K}}_{am} \\ \overline{\mathbf{K}}_{ma} & \mathbf{K}_{mm} \end{bmatrix} = \begin{bmatrix} \mathbf{T}_s^{fT}\mathbf{K}_{ss}\mathbf{T}_s^f + \overline{\mathbf{K}}_i & \mathbf{T}_s^{fT}\mathbf{K}_{sm} \\ \mathbf{K}_{ms}\mathbf{T}_s^f & \mathbf{K}_{mm} \end{bmatrix} \tag{29}$$

5. Numerical Examples

Square plates with central crack subjected to bending, twisting and shear load as shown in Figure 5 will be solved by the present FFEM. The Poisson's ratio is assumed to be 0.3 for all the cases. The influence of the finite boundaries to the moment intensity factors will be discussed in details.

5.1 Plate with a crack subjected to bending moment

Consider a single crack in plate subjected to pure bending, Sih *et al.* (1962) using the Kirchoff's theory determined the analytical result for an infinite plate with a central crack. The moment intensity factor K_I was expressed as,

$$K_I = M_0 \sqrt{a} \tag{29}$$

where M_0 is the applied moment and a is the crack length. For plate with finite width w, the moment intensity factors against the ratio a/w were determined by Wilson and Thompson (1971), Chen and Chen (1984), and Liu and Jiang (2000) using conventional finite element method, hybrid displacement finite element method and global-local finite element method respectively. In this paper, FFEM was used to solve this problem. Because of symmetry, a quarter of the plate was used in the analysis, and it was divided into around 170 nodes and 270 triangular elements. Figure 6 depicts a typical mesh configuration for the crack length ratio (a/w=0.05). Figure 7 shows a plot of the moment intensity factors determined by FFEM and by other methods. It is observed that the results provide by FFEM agree well with the other researchers. The maximum derivation with the other results is less than 7 %.

5.2 Plate with a crack subjected to pure torsion

Sih *et al.* (1962) had analytically solved an infinite plate with a central crack subjected to uniform torsion T_0. The moment intensity factor K_{II} was expressed as,

$$K_{II} = T_0 \sqrt{a} \tag{30}$$

Zehnder and Hui (1994) reviewed the same problem using a trial displacement function which could satisfy the stress boundary conditions at crack surfaces and at the remote boundary. Exact solution of both the cracked and uncracked plate problems were solved. None of the stresses near the crack tip were found to be singular, thus K_{II} should be equal to zero. Finite plates with crack width ratio a/w ranged form 0.05 and 0.6 subjected to uniform twisting were calculated by using FFEM. All the moment intensity factors K_{II} were found to be zero. It is noted that similar problems were solved by other researchers utilizing the incorrect analytical results of Sih using finite element alternative approach [Chen and Shen, 1993] and global-local method [Liu and Jiang, 2000], none of the methods could give the correct solution of K_{II}=0.

5.3 Plate with a crack subjected to shear force

Consider a single crack in an infinite plate subjected to different arrangement of shear force Q_0 as shown in Figure 5a and 5b. Sih *et al.* (1962) determined the moment intensity factors K_I and K_{II},

$$K_I = \frac{8\nu Q_0 a^{3/2}}{6} \text{ and } \quad K_{II} = \frac{8Q_0 a^{3/2}}{6} \tag{31}$$

Those solutions were found to be incorrect by Zehnder and Hui (1994) using the complex variable method. The corrected moment intensity factors are

$$K_I = \frac{\nu Q_0 a^{3/2}}{2} \text{ and } \quad K_{II} = \frac{Q_0 a^{3/2}}{2} \tag{32}$$

Though this classical problem has been investigated for more than forty years, very few numerical solutions on this problem could be found in the literature. One of the examples is Viz *et al*. (1995) who used the finite element method to solve the problems and employed the virtual crack extension technique and nodal release technique to determine the moment intensity factors. Errors arranged from 0.1 to 3.6% were reported. However, the influence of finite boundaries on the computation of moment intensity factors was not discussed. This problem was considered by FFEM, the results of mode I and II moment intensity factors against various crack width ratio *a/w* are plotted in Figure 8 and Figure 9 respectively. The present results are in closed agreement with these by Zehnder despite that the solutions of infinite plate are comparing.

6. Conclusions

The formulation of the fractal finite element method to cracked plate by using Kirchhoff's theory has been discussed. The proposed method utilized the property of shape similarity of DKT element and fractal transformation technique to transform the infinite number of nodal displacements around the crack tip to a new set of generalized displacements. The number of unknowns could be reduced significantly and the moment intensity factor could be obtained directly from the generalized displacements. No other post-processing technique or interpolation method is required to determine the moment intensity factors. Examples of mode

I and mode II problems related with cracked plates subjected to bending, twisting and shear loads are provided. The influence of finite boundaries on the computation of moment intensity factors is studied in details. This study demonstrated that the FFEM is accurate and reliable to solve both mode I and mode II cracked thin plate problems.

7. Acknowledgement

The work described in this paper was fully supported by the grant from the Research Grants Council of the Hong Kong Special Administrative Region, China (Project Nos. HKU 7014/00E). The numerical examples and the graphs prepared by Mr. Paris Wong were also gratefully thanks.

8. References

Ahmad, J and Loo, F.T.C. (1979). Solution of plate bending problems in fracture mechanics using a specialized finite element technique, Engineering Fracture Mechanics, **11**, 661-673.

Chen, W.H. and Chen, P.Y. (1984). A hybrid-displacement finite element model for the bending analysis of thin cracked plates, *International Journal of Fracture*, **24**, 83-106.

Chen, W.H., Yang, K.C. and Chang, C.S. (1992). A finite element alternating approach for the bending analysis of thin cracked plates, *International Journal of Fracture*, **56**, 93-110.

Chen, W.H. and Shen, C.M. (1993). A finite element alternating approach to bending of thin plates containing mixed mode cracks, *International Journal of Solids and Structures*, **30**(16), 2261-2276.

Hui, C.Y. and Zehnder, A.T. (1993). A theory for the fracture of thin plates subjected to bending and twisting moments, *International Journal of Fracture*, **61**, 211-229.

Leung, A.Y.T. and Su, R.K.L. (1996). Fractal two-level finite element method for cracked classical plates using DKT elements, *Engineering Fracture Mechanics*, **54**(5), 703-711.

Liu, C.T. and Jiang C.P. (2000). *Fracture Mechanics for Plates and Shells*, National Military Industry press, Beijing. (In Chinese)

Murakami, Y. (1987). *Stress Intensity Factors Handbook*, Pergamon Press, Oxford.

Park, J.H. and Atluri, S.N. (1999). Analysis of a cracked thin isotropic plate subjected to bending moment by using FEAM, *KSME International Journal*, **13**(12), 912-917.

Sih, G.C., Paris, P.C. and Erdogan, F. (1962). Crack-tip, stress-intensity factors for plane extension and plate bending problems, *ASME, Journal of Applied Mechanics*, **29**, 306-312.

Sticklin, J.A., Haisler, W., Tisdale, P. and Gunderson, R. (1969). A rapidly converging triangular plate element, *AIAA Journal*, **7**(1), 180-181.

Su, R.K.L., Sun, H.Y. and Zhu, Y. (2001). Fractal finite element method for singular problems, *Proceedings of First Asian-Pacific Congress on Computational Mechanics, Sydney, Australia,* **1***, 20-23*, 655-660.

Timoshenko, S and Woinowsky-Krieger, S., (1959). Theory of Plates and Shells, MrGraw-Hill.

Viz., M.J., Potyondy, D.O., Zehnder, A.T., Rankin, C.C. and Riks, E. (1995). Computation of membrance and bending stress intensity factors for thin, cracked plates, *International Journal of Fracture*, **72**,21-38.

Williams, M.L. (1961). The bending stress distribution at the base of a stationary crack, *ASME Journal of Applied Mechanics*, **28**, 78-82.

Wilson, W.K., and Thompson, D.G. (1971). On the finite element method for calculating stress intensity factors for cracked plates in bending, *Engineering Fracture Mechanics*, **3**, 97-102.

Zehnder, A.T. and Hui, C.Y. (1994). Stress intensity factors for plate bending and shearing problems, Journal of Applied Mechanics, **61**, 719-722.

Zucchini, A., Hui, C.Y. and Zehnder, A.T. (2000). Crack tip stress fields for thin, cracked plates in bending, shear and twisting: A comparison of plate theory and three-dimensional elasticity theory solutions, *International Journal of Fracture*, **104**, 387-407.

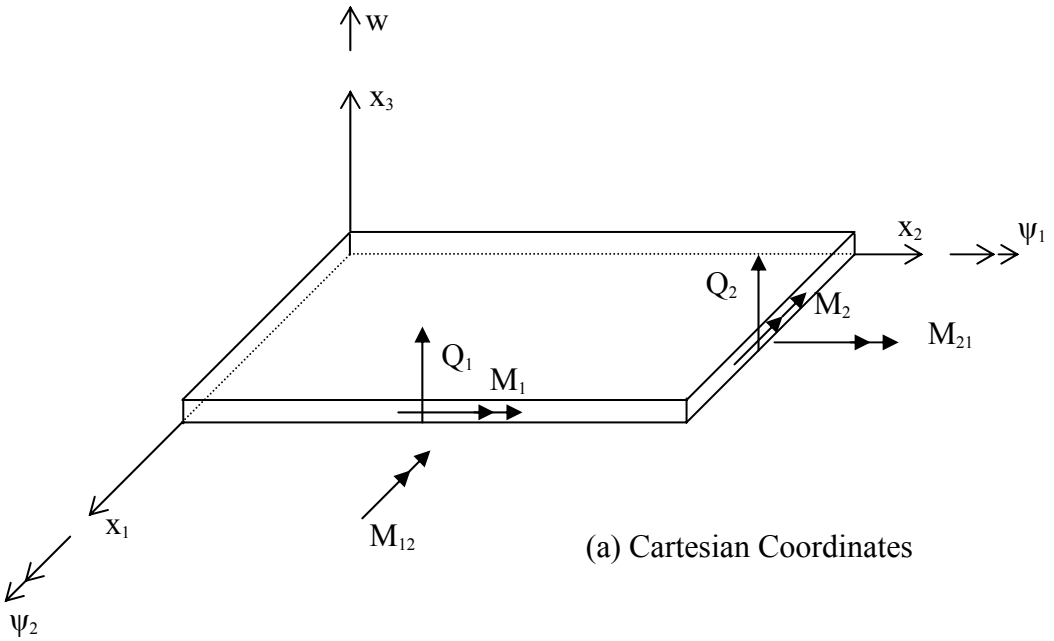

(a) Cartesian Coordinates

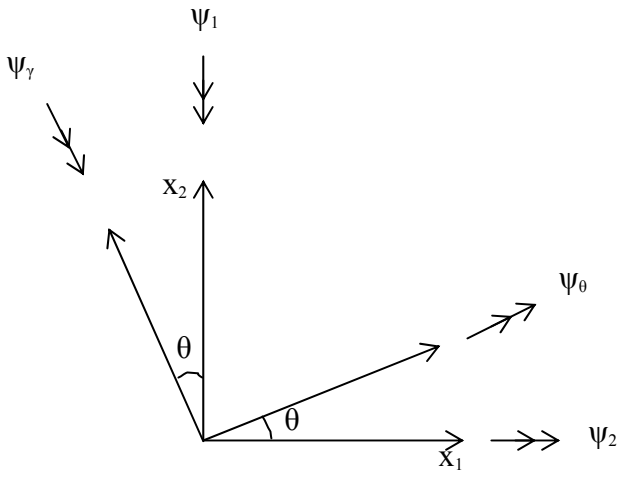

(b) Polar Coordinates

Figure 1. Notations for Kirchhoff's plate.

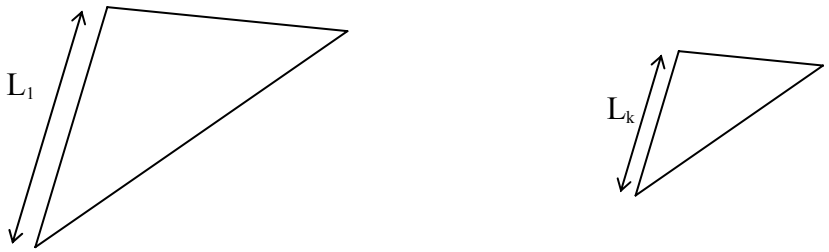

Element 1

Element k

Same thickness for element 1 and element k

Figure 2. Plate bending elements with similar shapes.

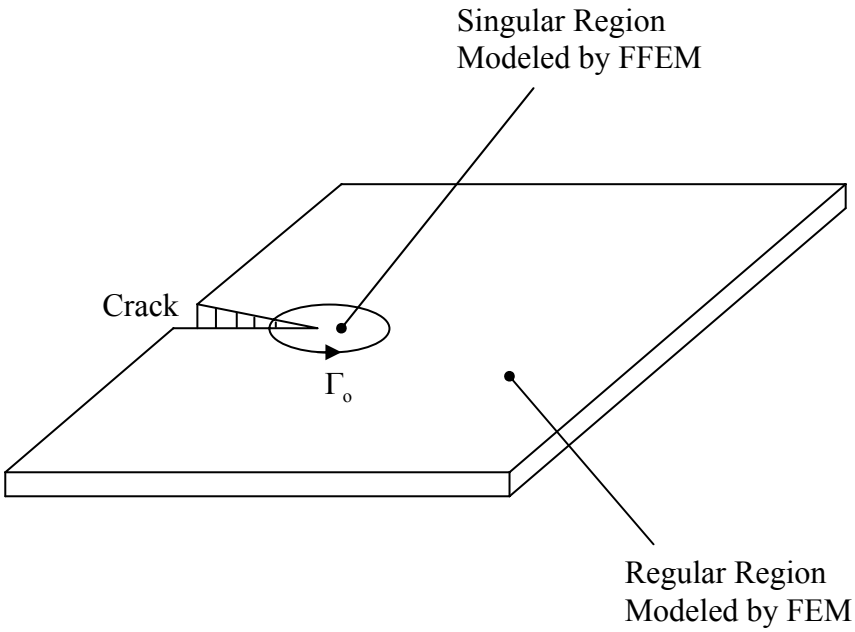

Figure 3. Singular and regular regions.

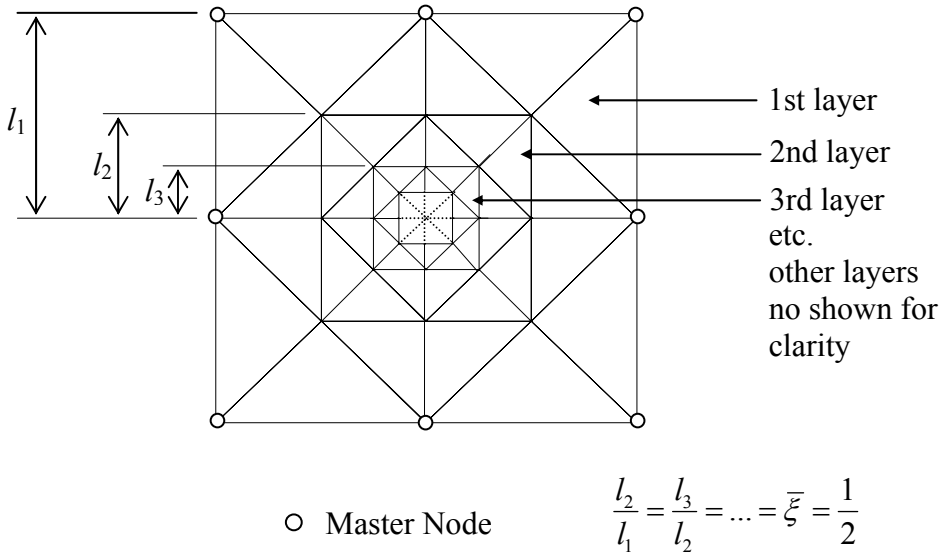

Figure 4. Fractal Mesh Configuration of Triangular Plate Elements.

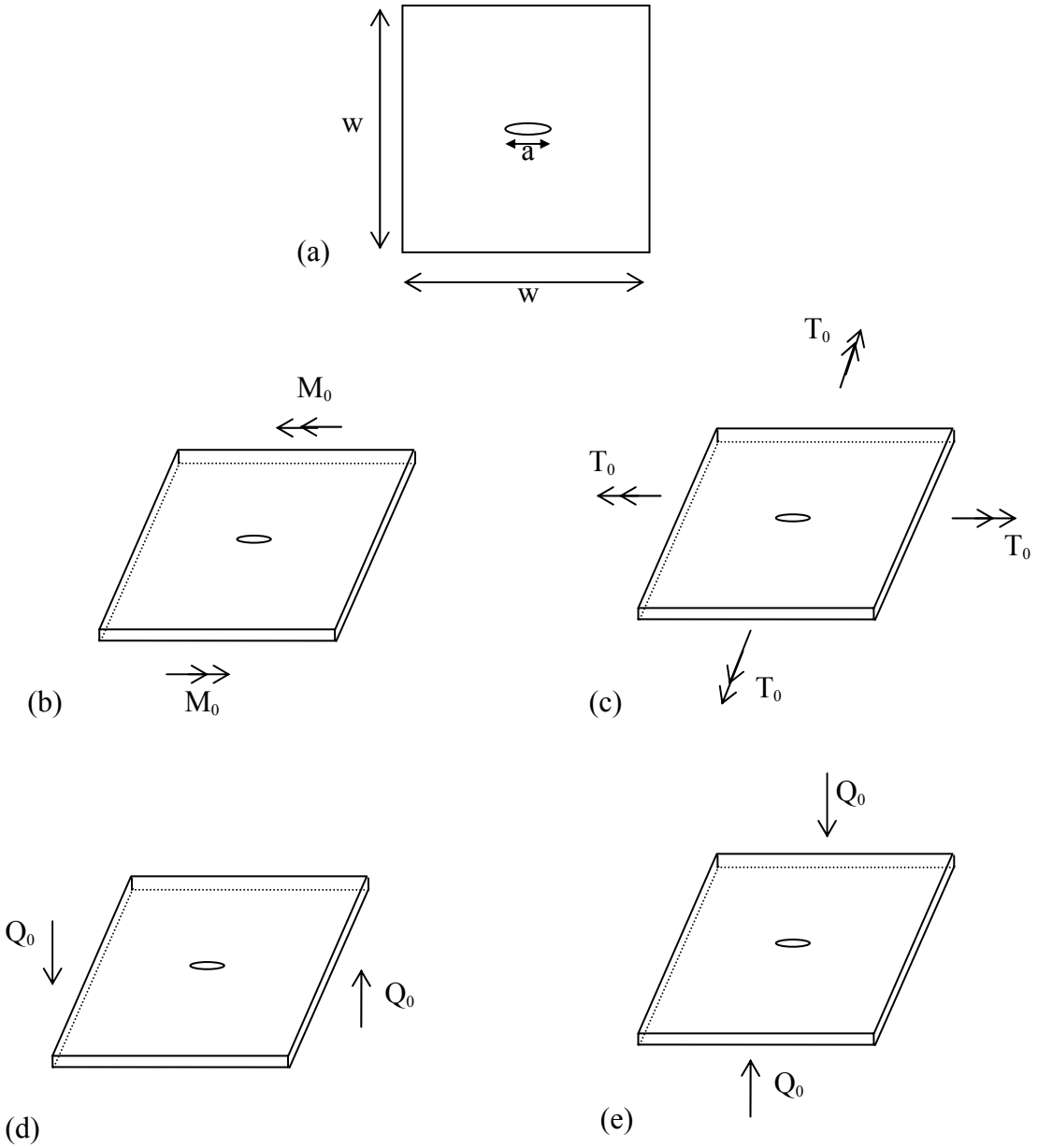

Figure 5. Problems of cracked plates studied by FFEM.

(a). Configuration of cracked plate.
(b). Cracked plate subjected to bending.
(c). Cracked plate subjected to torsion.
(d). Cracked plate subjected to shear (Mode I).
(e). Cracked plate subjected to shear (Mode II).

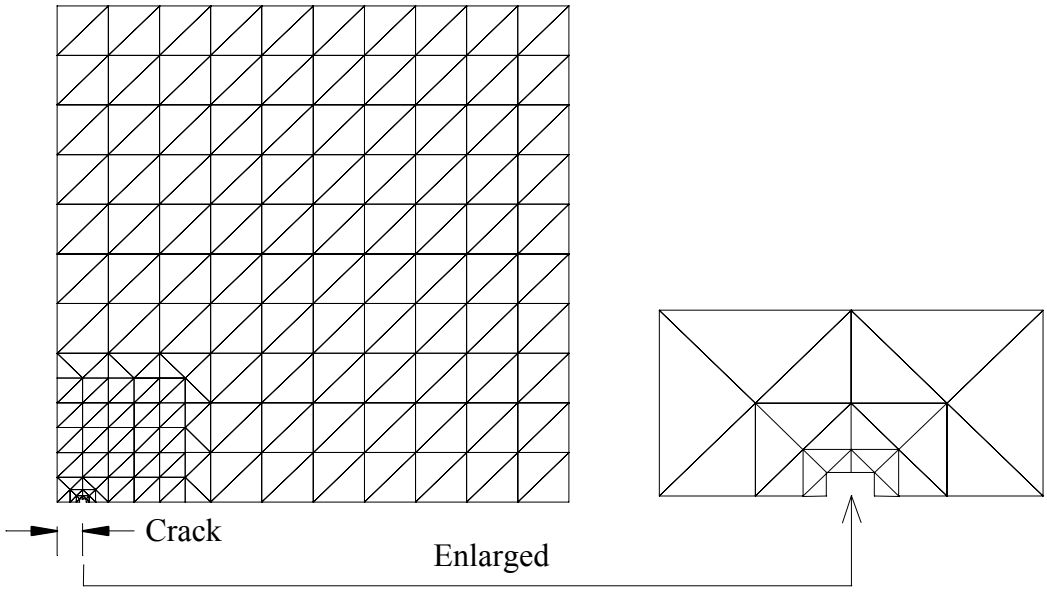

Figure 6. Mesh for center edge crack (a/w = 0.05).

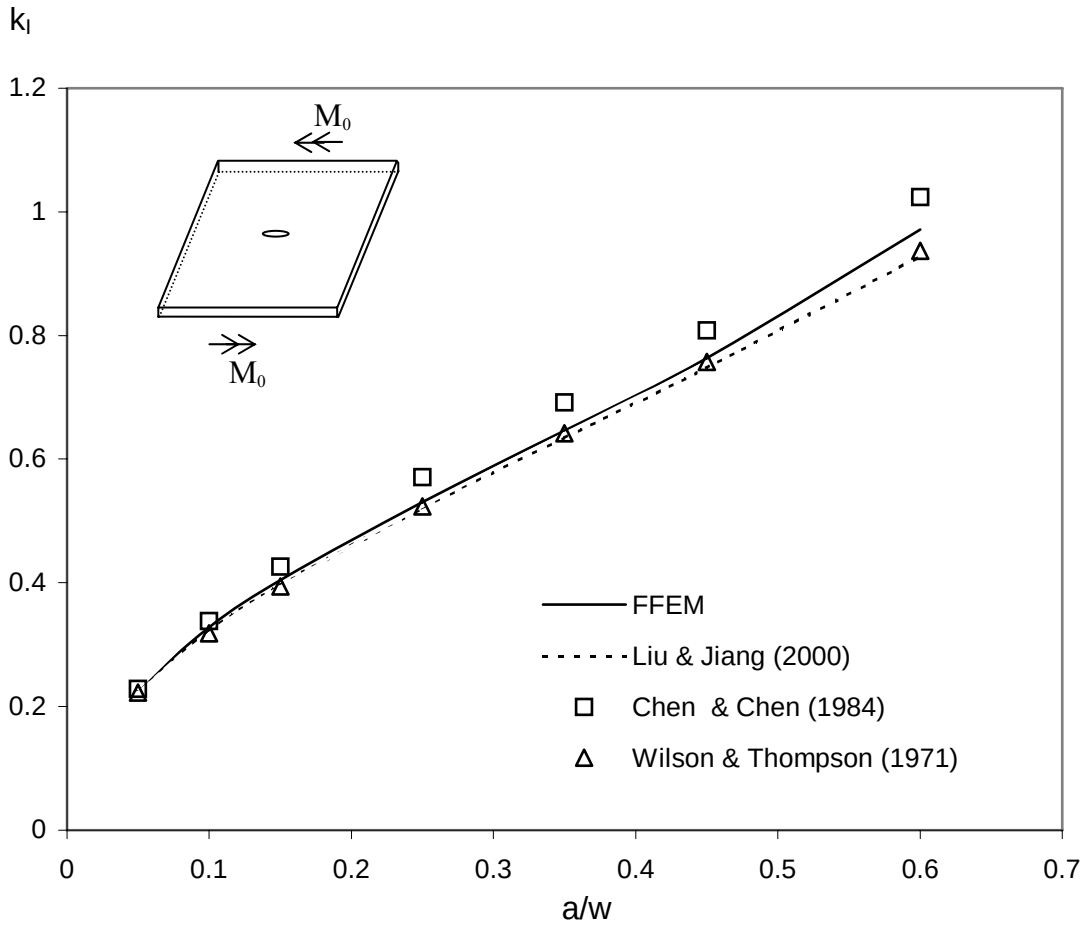

Figure 7. Moment intensity factors for a square plate with central crack subjected to bending moment

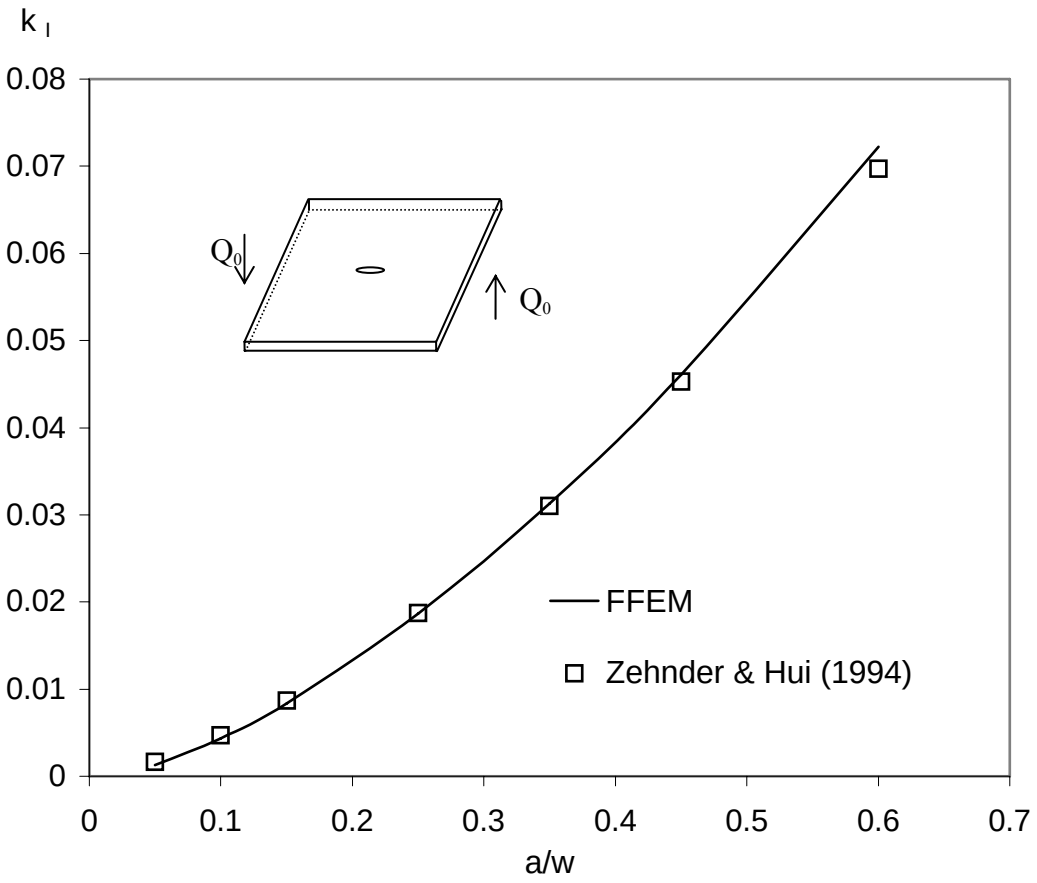

Figure 8. Mode I moment intensity factors for a square plate with central crack subjected to shear.

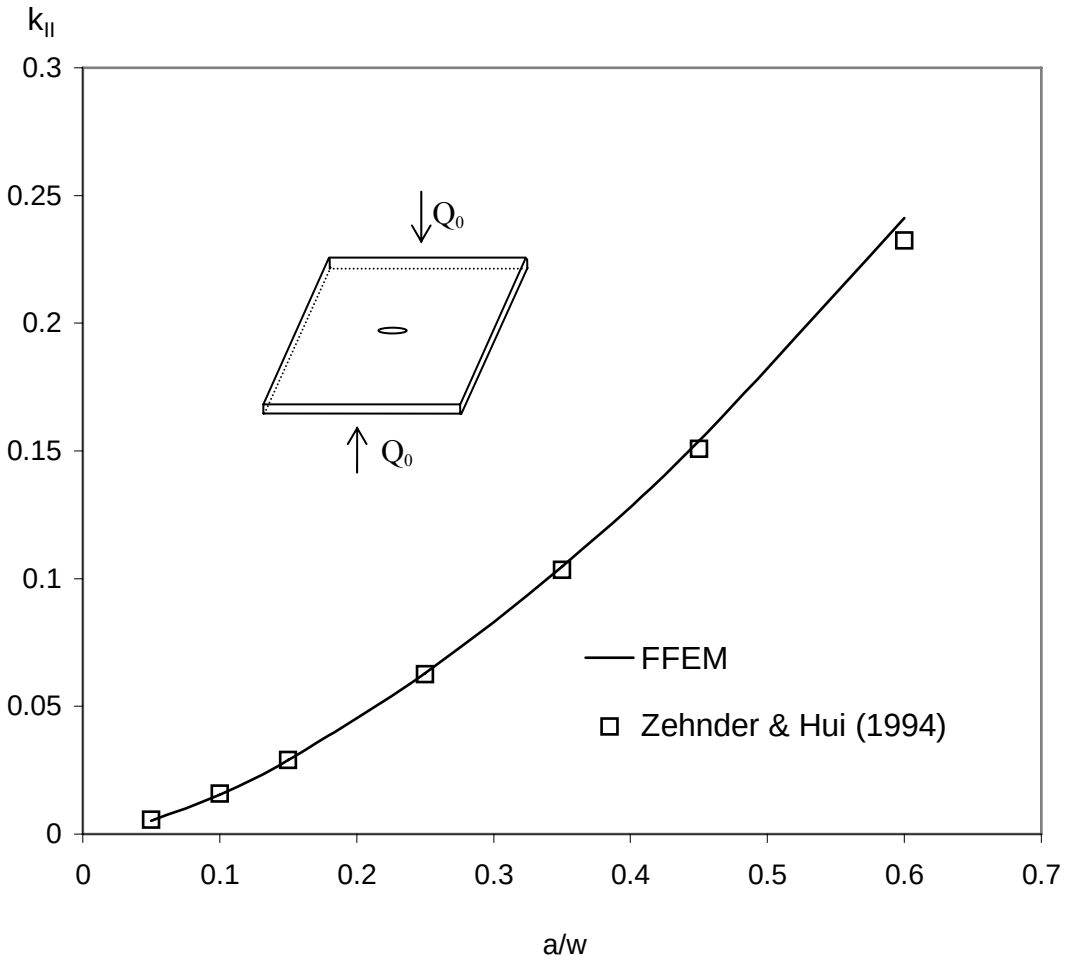

Figure 9. Mode II moment intensity factors for a square plate with central crack subjected to shear.